

Article

Biosorption of Aqueous Pb(II), Co(II), Cd(II) and Ni(II) Ions from Sungun Copper Mine Wastewater by *Chrysopogon zizanioides* Root Powder

Saba Madadgar^{1,2}, Faramarz Doulati Ardejani^{1,2,*} , Zohreh Boroumand^{1,3}, Hossein Sadeghpour¹, Reza Taherdangko^{4,*}  and Christoph Butscher⁴ 

¹ School of Mining Engineering, College of Engineering, University of Tehran, Tehran 1439957131, Iran

² Mine Environment and Hydrogeology Research Laboratory (MEHR lab), University of Tehran, Tehran 1439957131, Iran

³ Nano-Bio Earth Laboratory, Applied Geological Research Center of Iran, Karaj 3174674841, Iran

⁴ Institute of Geotechnics, TU Bergakademie Freiberg, 09599 Freiberg, Germany

* Correspondence: fdoulati@ut.ac.ir (F.D.A.); reza.taherdangkoo@ifgt.tu-freiberg.de (R.T.)

Abstract: In this study, a plant-based adsorbent was used in order to remove lead, nickel, cobalt and cadmium metals from a wastewater sample collected from Sungun mine real wastewater. The biosorbent was one of the most abundant native plants of the Sungun region, named *Chrysopogon zizanioides* (*C. zizanioides*). The root powder of *C. zizanioides* was used in order to remove heavy metals from the wastewater sample. The biosorbent was characterized by FTIR, SEM, HR-TEM, EDS, BET and ZPC analyses. The effect of pH, initial metals concentrations, contact time and temperature on the biosorption process were accurately investigated. The metal concentrations were significantly reduced to lower concentrations after the biosorption process, which indicated that the *C. zizanioides* root powder removal efficiency was more than 95% for the metals from the wastewater sample, with maximum adsorption capacities of 31.78, 21.52, 26.69 and 27.81 mg/g, for Pb(II), Co(II), Cd(II) and Ni(II) ions, respectively. Furthermore, the adsorption kinetic results showed that the pseudo-second-order kinetic model correlated with the experimental data well, with correlation coefficient values of 1 for all metals. Isotherm studies illustrated that the Freundlich and Dubinin-Radushkevich (D-R) isotherm models could describe the obtained equilibrium data well. Moreover, from the D-R model, it was found that the biosorption type was physical. The thermodynamic studies demonstrated that the metals' biosorption was an exothermic and spontaneous process. Moreover, the reusability of the biosorbent to be used in several successive cycles, and also the percentage of recovery of adsorbed metals from the biosorbent, was investigated. Altogether, being simple and cost-effective and having a high adsorption rate, fast kinetics, easy separation and high reusability prove that *C. zizanioides* root powder shows significant performance for the removal of heavy metals from waste effluents.

Keywords: equilibrium; kinetics; thermodynamic; biosorbent; *C. zizanioides*



Citation: Madadgar, S.; Doulati Ardejani, F.; Boroumand, Z.; Sadeghpour, H.; Taherdangko, R.; Butscher, C. Biosorption of Aqueous Pb(II), Co(II), Cd(II) and Ni(II) Ions from Sungun Copper Mine Wastewater by *Chrysopogon zizanioides* Root Powder. *Minerals* **2023**, *13*, 106. <https://doi.org/10.3390/min13010106>

Academic Editor: María

Ángeles Martín-Lara

Received: 29 November 2022

Revised: 23 December 2022

Accepted: 5 January 2023

Published: 9 January 2023



Copyright: © 2023 by the authors. Licensee MDPI, Basel, Switzerland. This article is an open access article distributed under the terms and conditions of the Creative Commons Attribution (CC BY) license (<https://creativecommons.org/licenses/by/4.0/>).

1. Introduction

With the rapid and progressive growth of anthropogenic activities, e.g., chemical industries, metal smelting and extraction, the manufacturing of electrical equipment, alloys and mining around the world, the environmental pollution of heavy metals has become a serious issue in the world [1]. One of the significant indicators of development in any society is to access safe drinking water. Heavy metals in polluted waters and industrial effluents, if not treated, can enter the food chain of animals and humans directly [2]. The US Environmental Protection Agency (EPA) considers some metals to be beneficial for human health in minor quantities [3]. On the other hand, many elements not only are unnecessary but are also considered a threat to the life of living organisms and may cause adverse effects on living beings. Among all existing metals, lead, nickel, cadmium and cobalt are some

of the most hazardous materials, especially in high concentrations, as they are toxic for most life forms and cannot be detoxified biologically [4,5]. The permissible limit for Pb(II) in wastewater given by the WHO is 0.05 mg/L [6,7]. The presence of lead in drinking water, even at below the permissible concentration, may cause anemia, encephalopathy and nephritic syndrome. In addition, the presence of cadmium, nickel and cobalt in drinking water may cause different toxicological effects on humans including mental disorders, immune system deficiency, asthma and an increased risk of cancer [8]. Hence, the removal of these elements from water is essential to protect humans and environmental health.

There are various conventional methods which are proposed for the removal of metals from water and wastewater, including chemical precipitation [9], hydroxide precipitation [10], sulfide precipitation [11], electrochemical methods [12], ion exchange [13], reverse osmosis [14] and adsorption [15]. Most of the wastewater treatment methods, in addition to high maintenance or operational costs, may have disadvantages such as the partial removal of certain ions, high power consumption, and the generation of toxic sludge and other wastes, which need to be disposed of [16]. However, the adsorption process is the most popular method, because it is an efficient, economical, easily accessible, sustainable, and eco-friendly method for removing organic and inorganic contaminants from polluted water [17]. In general, adsorbents can be in the types of activated carbon [18], synthetic polymers [19], silica-based adsorbents [20] and natural adsorbents. However, these types of adsorbents are rarely used for the treatment of wastewater, due to their high costs [21]. Using different biomaterials for the treatment of aqueous solutions has recently been paid more attention. The use of originally natural adsorbents has gained immense credibility because of their good performance, high uptake capacity, being cost-effective and being environmentally friendly [22].

Several previous works have reported the successful removal of metal ions from aqueous solutions and wastewater using different biosorbents. For instance, in a research study, 97.8% of lead was favorably removed in 49 min from an aqueous solution with an initial lead concentration of 93.5 mg/L, by *Henna* powder [23]. Lead was also removed by *Sargassum Tennerium* with 6.657 mg/g adsorption capacity [24]. Scientists achieved 14 mg/g adsorption capacity in the removal of nickel from aqueous solutions onto *Pistachio* hull waste as a biosorbent [25]. Moreover, nickel, lead and cadmium were effectively removed from contaminated water by *Camellia Sinensis* with 1.163, 1.197 and 2.468 mg/g adsorption capacities, respectively [26]. Furthermore, the removal percentage of cadmium and lead with initial concentrations of 5 mg/L from aqueous solutions were 92.76% and 94.09%, respectively, with modified *Spirulina Platensis*, and 87.52% and 90.09% with *Chlorella Vulgaris*, respectively [27]. In addition, cobalt with an initial concentration of 20 mg/L was removed by 98.7% using *Ficus Benghalensis* [28]. Zaidi et al. investigated the utilization of *Artocarpus odoratissimus* (Tarap) leaves for the removal of malachite green (MG) dye from simulated wastewater. A maximum adsorption capacity of 254.93 mg g⁻¹ was achieved. The biosorbent showed slight effects on the changes in the pH and ionic strength of the medium, which introduced it as a suitable adsorbent to be used in wastewater treatment. In addition, the artificial neural network model presented by the authors supported the experimental data and was able to accurately predict the effects of some parameters on the biosorption process [29]. Masinire et al. investigated the phytoremediation of Cr(VI) in wastewater using *C. zizanioides* by evaluating the effects of parameters such as the initial concentration, grass density and solution pH. The best results showed the remediation of Cr(VI) under acidic conditions with 100% removal in 20 days for the 30 ppm solution [30]. Kooh et al. presented an aquatic plant, *Azolla pinnata* (AP), for the adsorption of methylene blue (MB) dye. The adsorption process was modeled, applying several various supervised machine learning (ML) algorithms, including artificial neural network (ANN), random forest (RF), support vector regression (SVR), and instance-based learner (IbK). Among the different supervised machine learning algorithms, SVR-RBF proved to be the best algorithm with the highest R value (0.994) and the lowest error [31]. Weshahy et al. investigated the selective recovery of Cd, Co and Ni elements from spent Ni–Cd batteries using an Adogen[®]

464 solvent and mesoporous silica derivatives. Adogen 464 was used to extract Cd^{2+} by precipitating Cd as a yellow CdS product with 0.5% Na_2S solution at pH 1.25 at room temperature. PTU-MS silica adsorbent was used as an ion exchanger for Co^{2+} ions. Briefly, 0.3 M H_2SO_4 was used as an eluant, and Co was precipitated in the form of $\text{Co}(\text{OH})_2$ compound at up to pH 9.0. Finally, Ni was directly precipitated at pH 8.25, applying a 10% NaOH solution at ambient temperature [32]. Lu et al. studied the plant growth-promoting (PGP) characteristics of multi-metal-tolerant *Bacillus cereus* and their positive role on the phytoremediation capability of *C. zizanioides* in a soil sample contaminated with Cd, Zn, Pb, Mn and Cr. The growth and phytoremediation ability of *C. zizanioides* on metal-contaminated soil were improved by *Bacillus cereus* species. The maximum absorption capacity of *C. zizanioides* with *Bacillus cereus* was 12.15, 16.72, 11.47, 14.52 and 7.74 mg g^{-1} for Cd, Zn, Pb, Mn and Cr, respectively [33].

C. zizanioides is a native perennial plant of some regions of Asia that has high resistance against drought and pests. The root system of *C. zizanioides* is finely structured and very strong [34]. Under high-velocity flows, the root system protects *C. zizanioides* from being displaced [35]. Furthermore, it is able to survive in harsh conditions, and this feature has increased its range of tolerance against different pollutions [36]. The high tolerance of a range of extreme soil conditions is a significant feature of *C. zizanioides*, especially in contamination with heavy metals. Field experiments have also demonstrated that *C. zizanioides* can prosper under a wide range of pHs, and it is very persistent to saline and sodic soil situations [37].

Accordingly, the biosorbent used in the present investigation exhibits the following novel features: (1) available in abundance; (2) self-growing; (3) cost-effective; (4) simple; and (5) excellent ability in the removal of toxic metal ions from aqueous solution, which can play a valuable role in the adsorption of heavy metals from water and soil.

The main objective of this study was to use native plants of a region to remove some metal ions from that region's wastewater. For this purpose, the most abundant and available native plant of the Sungun region, which is called *C. zizanioides*, was used, and its performance as a natural adsorbent to remove heavy metals from the wastewater of the region was investigated.

2. Materials and Methods

2.1. Chemicals

The chemicals utilized in this study are as follows: HNO_3 , $\text{Pb}(\text{NO}_3)_2$, NiCl_2 , $\text{Co}(\text{NO}_3)_2$ and $\text{Cd}(\text{SO}_4)$ and were purchased from the Merck company. All of the solutions that were used in the study were prepared using deionized water (18.2 $\text{M}\Omega\cdot\text{cm}$), and all of the reagents used were of analytical grade.

2.2. Sampling of Wastewater

The wastewater samples used for further experiments were collected two times per day for four days in a row in the fall from wastewater around the Sungun mine in the city of Varzaghan in northwestern Iran in order to measure how much of certain elements was in the sample. There were no pretreatment and preprocessing for the wastewater samples, as the pHs of the samples were measured as approximately between 5.5 to 6.0, and preservations such as acid digestion were not necessary. The initial measurements taken by ICP-MS indicated that the wastewater sample contained some heavy metals.

2.3. Biosorbent Preparation

The *C. zizanioides* grass was collected from local fields of Sungun, nearby the Sungun copper mine. According to the experiments carried out on different parts of the considered plant, such as the root and the stem, the root of the plant had a higher efficiency in adsorbing metals from wastewater, and as a result, the root of the plant was used for further experiments. Thus, the roots were separated from the stems, and the mud was removed from the roots. Afterwards, they were carefully washed with tap water followed

by distilled water to remove residual dirt. They were then dried at 30 °C in a hot air oven and converted into powder by a grinder, and then sieved to give a fraction of a 200 mesh screen. The resulting powder was used as a biosorbent for the subsequent tests without any pretreatment.

2.4. Characterization Studies

The biosorbent was characterized through several different analyses. Fourier transform infrared (FTIR) analysis is a method for identifying the functional groups present on each adsorbent surface and the compositions and constituent phases of the materials that play an important role in the biosorption efficiency. The functional groups of the *C. zizanioides* root may affect the biosorption process. They were characterized by an FTIR technique using an AVATAR (Thermo, Waltham, MA, United States) over a working range of 350–7800 cm^{-1} . Scanning electron microscopy (SEM) analysis was carried out in order to identify the surface morphology and chemical compounds of the biosorbent using a ZEISSEVO 18 scanning electron microscope. Moreover, the elemental compositions of the biosorbent were determined before and after the adsorption of the metal ions by an energy-dispersive spectrometer (EDS). The elements concentrations were determined by Inductively Coupled Plasma Mass Spectrometry (ICP-MS) using 7500, Agilent, Santa Clara, CA, United States. Brunauer–Emmett–Teller (BET) analysis was performed in order to calculate the surface areas, pore size distributions and pore volumes of the *C. zizanioides* root powders using a Microtrac BELSORP-mini over a working range of 0.35–200 nm and a relative pressure (p/p_0) of 133 KPa. High-resolution transmission electron microscopy (HR-TEM) analysis was carried out for the purpose of characterizing the biosorbents' physicochemical features and element distributions using an FEI-TEC9G20. Additionally, using the energy-dispersive spectrometry (EDS) method, the elemental analysis of the biosorbent was determined by the elemental analysis equipment installed on this device. The point of zero charge (PZC) of the biosorbent and the pH of the solutions were studied using a Metrohm 827 digital pH meter, working in a temperature range from -150 °C to $+250$ °C.

2.5. Adsorption Studies

In the batch system, in order to optimize the toxic metal ion (lead, nickel, cobalt and cadmium) removal, the effects of the experimental conditions, including the adsorbent dosage, pH, initial ion concentration, temperature and contact time on the adsorption process were studied. The experimental procedure involved the following steps:

- (1) The wastewater sample was collected from wastewater around Sungun mine in order to measure the amount of certain elements by ICP-MS.
- (2) A weighed amount of the biosorbent (100 mg/L) was added to the sample solution.
- (3) The wastewater sample was transferred into 100 mL Erlenmeyer flasks and was shaken in a FineTech-SKIR-601 shaking incubator at 250 rpm.
- (4) For the purpose of investigating the kinetic studies and the effect of contact time, a series of flasks containing 100 mg/L of the biosorbent and 100 mL of the wastewater sample were shaken for different time intervals (5–120 min), at a constant speed of 250 rpm and a constant temperature of 298 K. Then, pseudo-first-order, pseudo-second-order kinetic and intra-particle diffusion models were used to analyze the experimental data.
- (5) Isotherm experiments were carried out at different initial concentrations (0.1–10 mg/L) of lead, nickel, cobalt and cadmium ions and shaking in 100 mL of the sample solution for an equilibrium time and at a constant temperature of 298 K. In order to prepare solutions with lower and higher concentrations than the main wastewater sample, certain weighed amounts of $\text{Pb}(\text{NO}_3)_2$, NiCl_2 , $\text{Co}(\text{NO}_3)_2$ and $\text{Cd}(\text{SO}_4)$ were added to the solutions. The equilibrium solution concentration was measured, and the quantities of metals adsorbed per unit weight of biosorbent were calculated by the equilibrium equations. In addition, the biosorbent distributions between the solid

and liquid phases were assessed by different isotherm models including Langmuir, Freundlich and Dubinin-Radushkevich isotherm models.

- (6) To carry out thermodynamic studies and investigate the effects of temperature on the biosorption process, 100 mL of the desired solution containing 100 mg/L of biosorbent, with initial concentration of each metal and 5 mg/L of each metal, and different temperatures (298, 313 and 323 K) was stirred for 2 hrs, at a constant speed of 250 rpm in a temperature-controlled shaking incubator. The thermodynamic studies were then carried out using the corresponding equations.
- (7) The amount of specific ions adsorbed by the biosorbent at equilibrium and the removal percentage were obtained using Equation (1) [38]:

$$q_e = \frac{(C_0 - C_e)V}{M} \quad (1)$$

where q_e is the adsorption capacity (mg/g) and C_0 and C_e are the initial and the final concentrations of the heavy metals (mg/L), respectively. V is the volume of the solution (L), and M is the mass of the used adsorbent (g).

- (8) The reusability of the biosorbent and the desorption performance were further investigated.

2.6. Desorption Experiments

Desorption studies are of great importance to check the stability of adsorbent particles in acidic environments, their reusability and also the recovery of metals. In order to investigate the desorption process of the metals, after completing the biosorption process, the biosorbent particles were separated by a filtration and centrifugation process after stirring for 120 min at a speed of 250 rpm. The separated biosorbent particles were then added to 100 mL of 0.15 M nitric acid solution. In order to check the stability and efficiency of the biosorbent during several stages of washing, all of the steps of this process were repeated in four cycles and all of the separated solutions were collected.

3. Results and Discussion

3.1. Characterization of Biosorbent

FTIR analysis was used to identify the surface functional groups and chemical compounds of *C. zizanioides* root. The FTIR spectra of *C. zizanioides* root powder both before and after the biosorption modes are given in Figure 1. The spectra show a number of characteristic biosorption peaks of *C. zizanioides* root powder within a range of the 400–4000 cm^{-1} wave number, which is composed of various functional groups. A broad peak at 3431 cm^{-1} is related to the overlapping of the –OH and –NH bonds [39]. Another peak at 2923 cm^{-1} could be attributed to the –CH stretching vibrations of the CH_3 and CH_2 functional groups [40]. Another peak at 1736 cm^{-1} was recorded in the spectrum, which was assigned to the carboxylate ion ($-\text{COO}^-$) [41]. One more peak at 1636 cm^{-1} was recorded in the spectrum and could be attributed to the C=O bonds of carboxylic acid and the presence of an amide group (protein) [39,42]. An additional sharp peak at 1036 cm^{-1} was recorded in the spectrum, which could correspond to the C–O bonds of alcohols and carboxylic acids [40].

After the biosorption process, several bands observed in the spectrum of the *C. zizanioides* root powder were shifted, and their shapes changed. Some bands showed a much greater intensity in their spectrum after biosorption. The peak of 3431 cm^{-1} was shifted to 3453 cm^{-1} . Changes in the adsorption intensity and changes in the wave number of functional groups can be due to the interaction of metal ions with the active sites of biosorbents [40,43].

SEM microscopic images of *C. zizanioides* root powder, before and after biosorption, at different magnifications, are shown in Figure 2a,b and Figure 2c,d, respectively. As depicted in Figure 2a,b, the material is irregular in shape and provides a large and accessible surface area and suitable binding sites for the metals' biosorption due to its porosity. In Figure 2c,d,

the SEM micrographs of the biosorbent after the biosorption process illustrate changes in the surface morphology of the biosorbent and show a less porous surface, which indicates the metals' biosorption to the binding sites of the biosorbent.

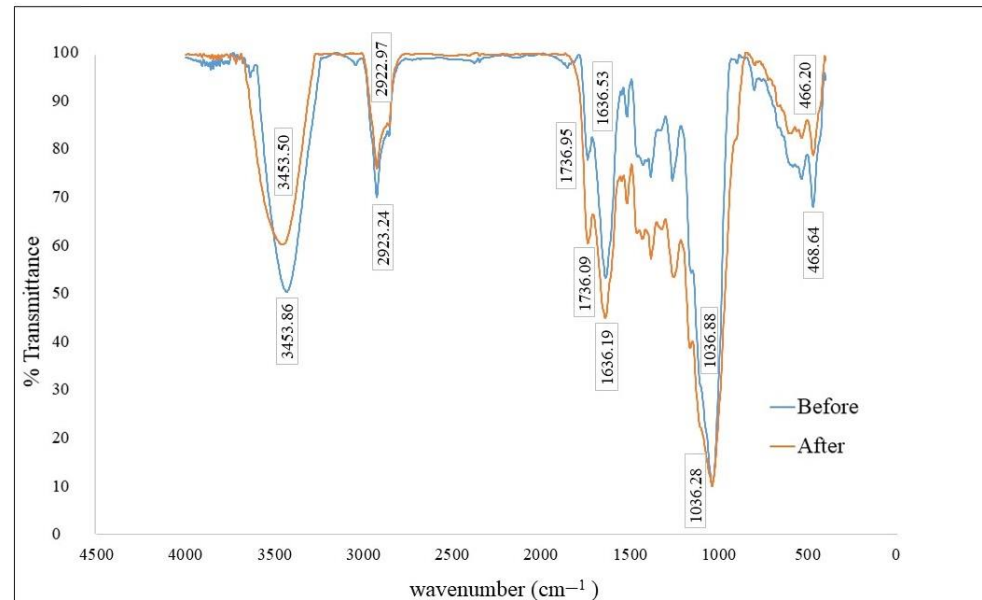


Figure 1. FTIR spectra for before and after the biosorption of the heavy metals by *C. zizanioides* root.

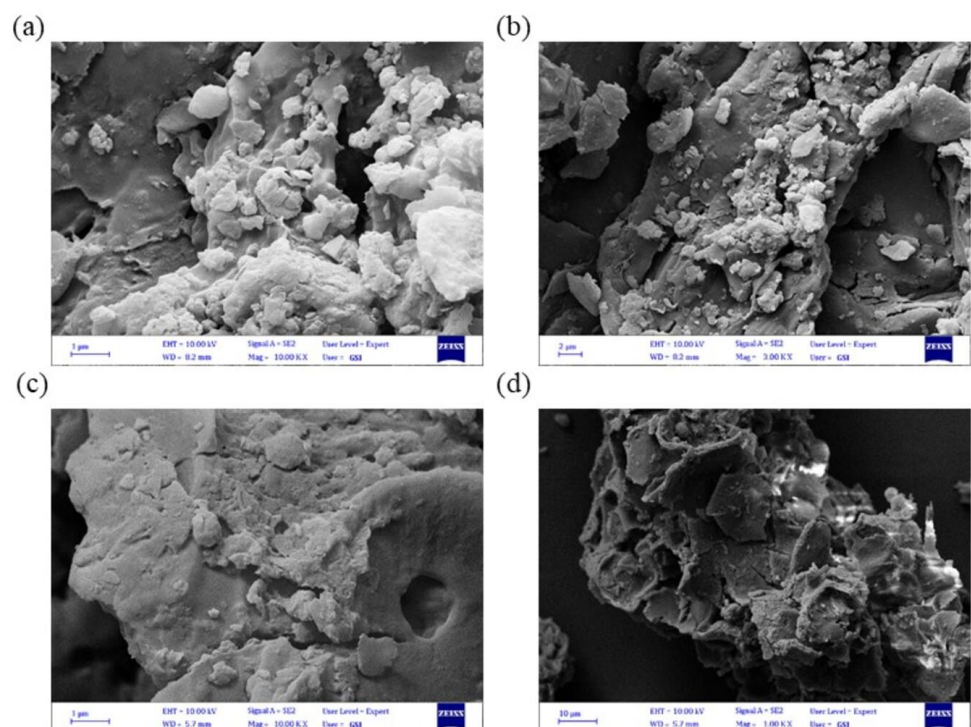


Figure 2. SEM images of *C. zizanioides* root; (a,b) before biosorption, (c,d) after biosorption.

The EDS spectra and the elemental compositions before and after the biosorption process are shown in Figure 3a,b, respectively. Based on Figure 3a, considering that the biosorbent was picked up from the native region, the biosorbent contains quantities of metals, including Pb, Ni and Cd, before biosorption. The results shown in Figure 3b indicate that the metal amounts increased after the biosorption process, which confirms the high

ability and significant performance of the biosorbent in the removal of heavy metals from wastewater.

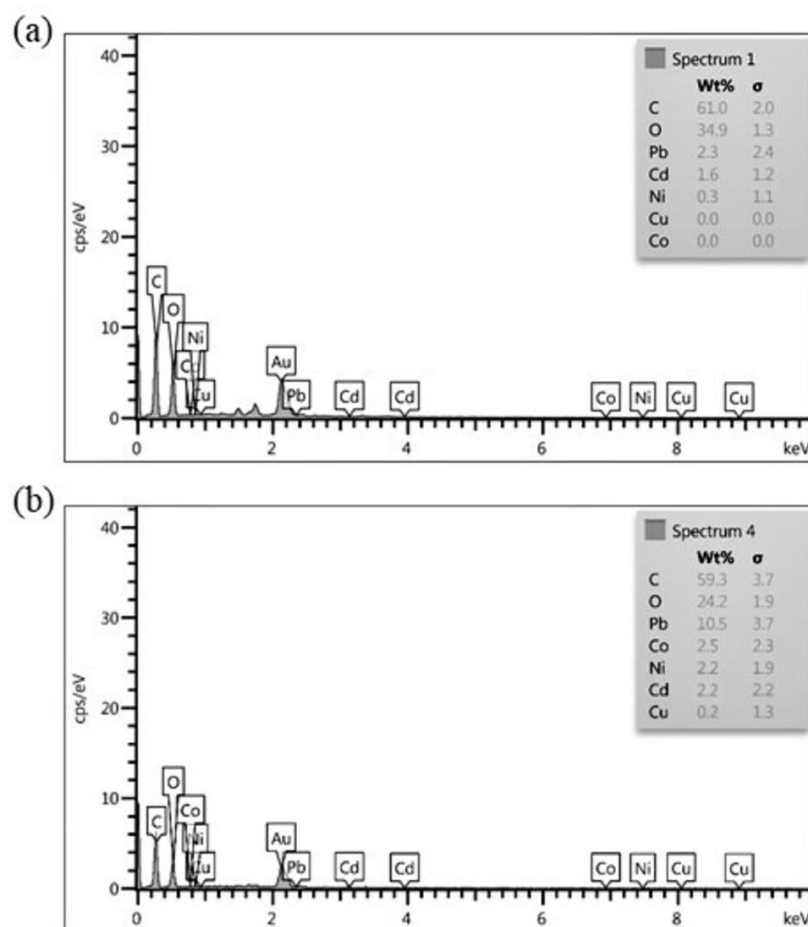


Figure 3. EDS analysis of *C. zizanioides* root; before (a) and after (b) biosorption.

Multiple-point BET analysis was carried out to evaluate the precise specific surface area of the biosorbent, which performs a considerable role in the biosorption process. The results of this analysis for *C. zizanioides* root powder are listed in Table 1. As shown, the specific surface area of *C. zizanioides* root powder is 8.21 m²/g, which is considered a good amount compared to similar biosorbents [21,44–47]. Moreover, according to the total volume and average diameter of the pores, the biosorbent can perform well. The results indicate that *C. zizanioides* root has a porous structure, which could facilitate the biosorption process [48].

Table 1. The results of BET analysis.

Adsorbents	BET Surface Area (m ² /g)	Total Pore Volume (cm ³ /g)	Average Pore Diameter (nm)
<i>C. zizanioides</i> root powder	8.21	0.0151	7.36

The high-resolution transmission electron microscopy method (HR-TEM) was performed to characterize the biosorbent physicochemical features, structure, morphology, texture properties and porosity. The HR-TEM images of different levels of magnifications are shown in Figure 4. As indicated, the biosorbent has a porous structure, which facilitates

the biosorption of elements. Furthermore, the darker parts in the images indicate the metals that are trapped in the pores of the biosorbent.

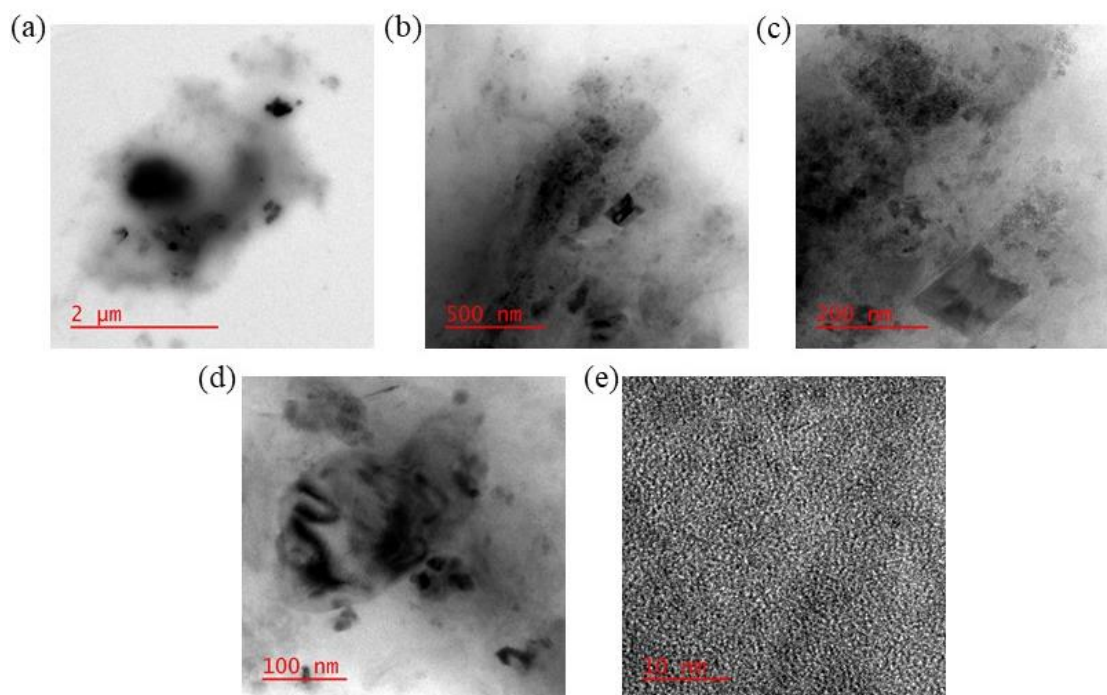


Figure 4. HR-TEM images of *C. zizanioides* root; (a) 2 μm ; (b) 500 nm; (c) 200 nm; (d) 100 nm; (e) 10 nm.

The point of zero charge (PZC) of the biosorbent was measured by measuring the pH at different pHs. As shown in Figure 5, the point of zero charge (pH_{zpc}) of the biosorbent is approximately 5.5, which indicates that the biosorbent surface charge is positive at pHs less than 5.5, and at pHs greater than 5.5, it is negative. Furthermore, it can be said that the biosorbent's most negative surface charge is at pHs between 6.0 and 7.0, which demonstrates that the biosorption process can be fully explained in this range of pHs.

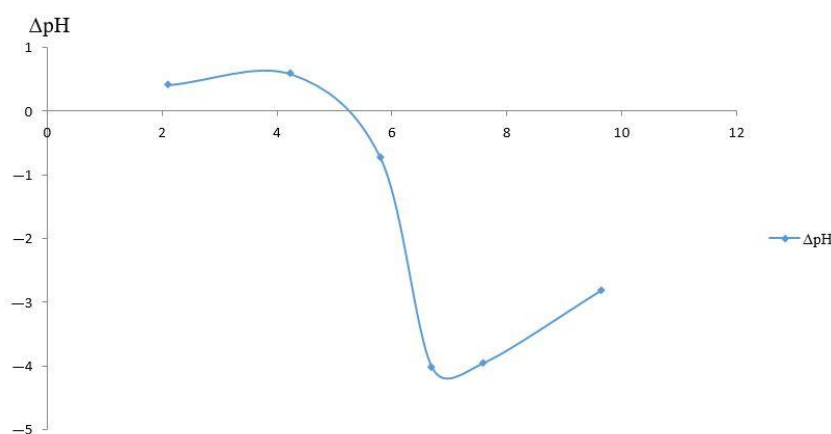


Figure 5. Point of zero charge of *C. zizanioides* root.

3.2. Sungun Wastewater

The chemical elements of the Sungun wastewater sample and its concentrations were measured before the biosorption process in order to assess the wastewater sample's quality and also evaluate the results after the biosorption process. The results of the ICP-MS analysis of the sample are shown in Table 2.

Table 2. The constituent elements and their concentrations in the Sungun wastewater sample [6].

Element	Pb	Ni	Cr	Co	Cd	As	Hg
Concentration (µg/L)	1462	2188	14.5	2085	1734	3.94	1.94
Permissible limit (µg/L) [6]	50	100	50	10	5	10	2

As can be observed in Table 2, the concentrations of lead, nickel, cobalt and cadmium in the wastewater were higher than their permissible limits [6], which confirms the significant necessity to eliminate these elements from the wastewater and prevent their discharge into natural water systems. The other coexisting elements were under the detection limit and not considered a threat to the environment and living beings.

3.3. Effect of pH

One of the effective parameters of the adsorption capacity is the pH of the reaction, which can directly control the reaction by changing the charges of the biosorbent and the metal ions. In order to determine the charges of the metal ions, the Eh–pH diagram was used [49]. Figure 6 indicates that all four desired elements are present as cations at a pH equal to 7.0 and an Eh equal to 0.18 volts. Our focus in this research was on the wastewater, and the desired pH was a neutral pH value. As the biosorbent’s most negative surface charge was at pHs between 6.0 and 7.0, the cations’ biosorption process by this biosorbent is well confirmed, with the negative surface charge of the biosorbent and the positive charge of cations at this pH, based on Eh–pH diagrams. Accordingly, no further pH experiments were required in order to determine the effect of pH on the biosorption reaction.

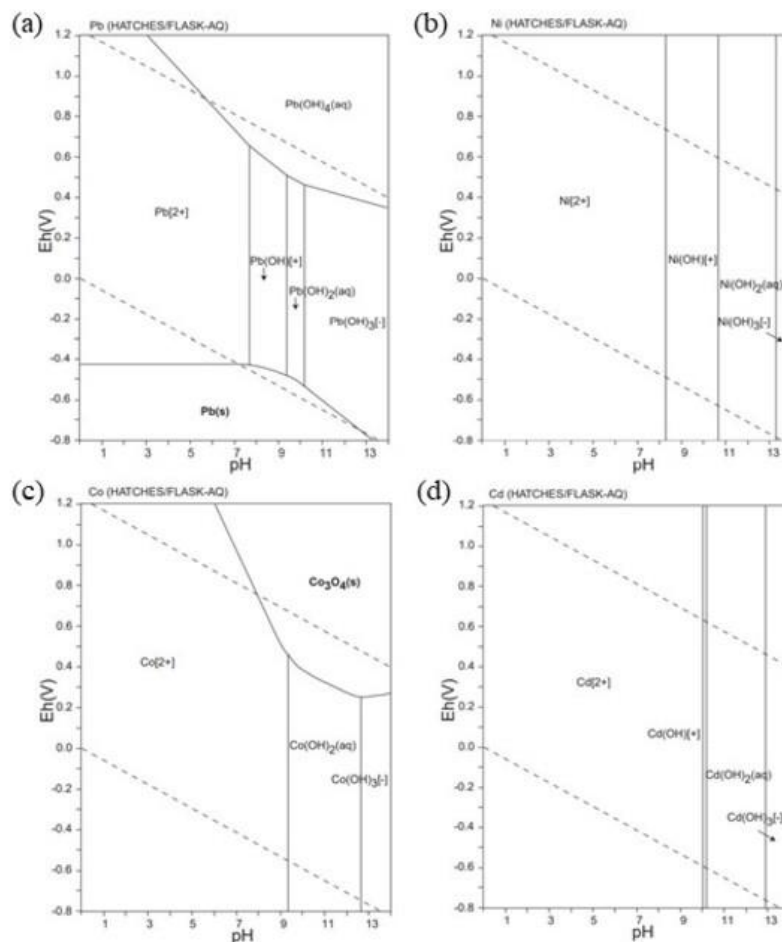


Figure 6. Eh–pH diagram of cobalt (a), nickel (b), cadmium (c) and lead (d) species [49].

3.4. Effect of Adsorbent Dosage

The adsorbent dosage is an important parameter that can affect the performance of the adsorption process and the adsorption capacity. It is essential to determine the optimum amount of the adsorbent dosage, as the removal efficiency can increase with higher adsorbent dosages. However, an excess adsorbent dosage may negatively affect the removal efficiency due to particle agglomeration, which may reduce the active sites for the adsorption process [50]. Figure 7 shows the effect of the adsorbent dosage on the biosorption capacity and removal efficiency. As can be observed, by increasing the adsorbent dosage from 50 mg/L to 3000 mg/L, the removal efficiency was found to be insignificant in such a way that increasing the adsorbent dosage did not have much effect on the removal efficiency of lead, nickel, cobalt and cadmium, and the changes were ignorable at doses higher than 0.1 mg/L. Consequently, the optimum adsorbent dosage was achieved at 0.1 mg/L for further experiments, which can be economically practical.

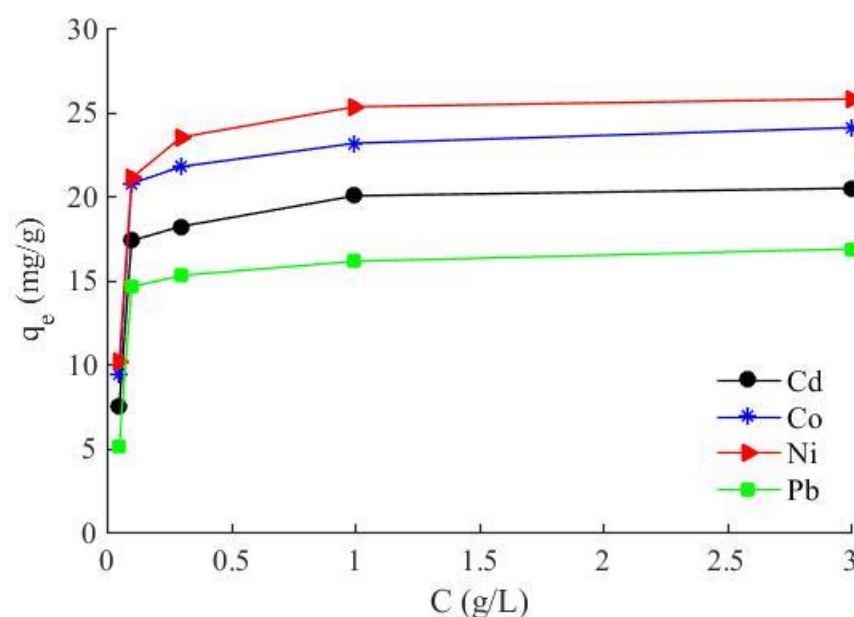


Figure 7. The effect of adsorbent dosage on the biosorption capacity (Pb, Ni, Co and Cd initial concentrations: 1.46, 2.19, 2.08 and 1.73 mg/L, respectively, adsorbent dosage: 50–3000 mg/L, volume of solution: 100 mL, time: 120 min, and $T = 298$ K).

3.5. Adsorption Kinetics and Effect of Contact Time

Adsorption kinetics have been studied in order to better understand the biosorption dynamics and provide a predictive model that allows to estimate the amount of adsorbed ions over the processing time. In order to better understand the adsorption mechanism, the various kinetics models including pseudo-first-order, pseudo-second-order and intra-particle diffusion models were applied to analyze the experimental data.

3.5.1. Pseudo-First-Order Model

The linear form of the Lagergren pseudo-first-order model is expressed based on Equation (2) [51]:

$$\ln(q_e - q_t) = \ln q_e - k_1 t \quad (2)$$

where K_1 (1/min) is the first-order kinetic constant and q_e (mg/g) and q_t (mg/g) represent the amount of substance adsorbed by the biosorbent at the equilibrium time and the time t , respectively.

3.5.2. Pseudo-Second-Order Model

The best-fit equations of the linear form of the pseudo-second-order kinetics can be expressed by Equation (3) [52]:

$$\frac{t}{q_t} = \frac{1}{K_2 q_e^2} + \frac{t}{q_e} \quad (3)$$

where $K_2(\text{g}\cdot\text{mg}^{-1}\cdot\text{min}^{-1})$ is the pseudo-second-order rate constant.

3.5.3. Intra-Particle Diffusion Model

In addition to the adsorption on the outer layer of the adsorbent, it is possible that metal ions diffuse into the adsorbent particles through the pores of the adsorbent surface. This is because adsorption is a multi-stage process involving the transfer of soluble particles from the aqueous phase to the surface of solid particles and then the penetration and diffusion of adsorbed molecules into the pores. Weber and Morris suggested an intra-particle diffusion model to consider pore diffusion that can be expressed by Equation (4) [53]:

$$q_t = C + K_i \sqrt{t} \quad (4)$$

where q_t is the intra-particle diffusion parameter and shows the amount of solute adsorbed, $K_i(\text{mg}\cdot\text{g}^{-1}\cdot\text{min}^{-0.5})$ represents the intra-particle diffusion model constant and C is refers to the adsorption constant and provides information about the thickness of the boundary layer.

In order to determine the processes that control the biosorption process, investigate the biosorption rate and find the correct time to operate the biosorption, kinetic studies were carried out. The amounts of Pb, Ni, Cd and Co biosorption on the biosorbent as a function of time are shown in Figure 8. As can be seen, the biosorption occurred at a high speed, and the maximum biosorption rate was achieved within 5 min for *C. zizanioides* root powder. It indicates that an extremely high biosorption rate is accessible in a short time. Although a period of 5 min is enough for biosorption, in order to achieve 100% equilibrium, the required time was considered up to 2 h for further experiments to continue the biosorption processes.

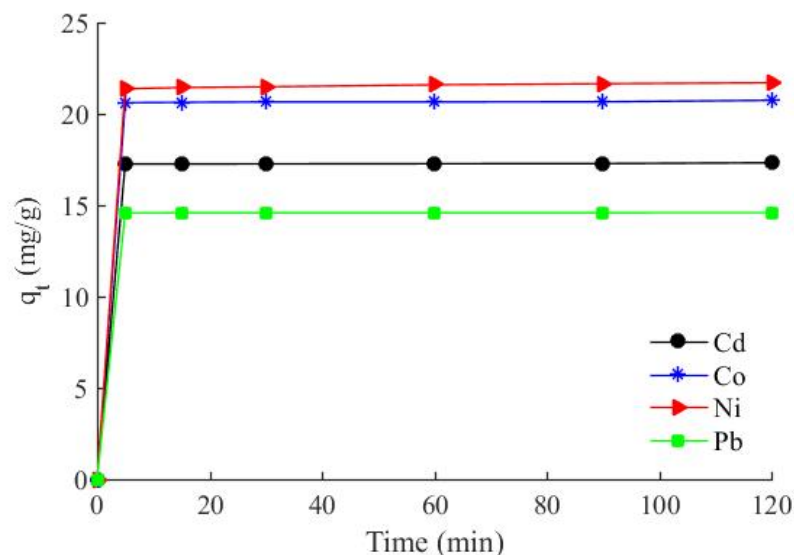


Figure 8. Effect of contact time on the biosorption (Pb, Ni, Co and Cd initial concentrations: 1.46, 2.19, 2.08 and 1.73 mg/L, respectively, adsorbent dosage: 100 mg/L, volume of solution: 100 mL, time: 5–120 min, $T = 298 \text{ K}$, $\text{pH} = 7.0$).

Based on the obtained results in Table 3, it can be definitely said that pseudo-first-order and intra-particle diffusion kinetic models were less successful in predicting biosorption

kinetics compared to pseudo-second-order models by giving the values of correlation coefficients ($R^2 = 1$). Therefore, it can be said with certainty that the pseudo-second-order kinetic model is the best-fitting model to describe the biosorption mechanism of these four metals, which assumes that the rate of occupation of the adsorption sites is in proportion to the square of the number of unoccupied sites [21].

Table 3. Adsorption kinetics parameters for Pb, Ni, Co and Cd (initial concentrations were 1.46, 2.19, 2.08 and 1.73 mg/L, respectively).

Element	1st Order Plot: $\ln(q_e - q_t)$ vs. t $q_e = \exp(\text{intercept})$ $k_1 = -\text{slope}$			2nd Order Plot: t/q_t vs. t $q_e = 1/\text{slope}$ $k_2 = \text{slope}^2/\text{intercept}$			Intra-Particle Diffusion Plot: q_t vs. $t^{0.5}$ $K_i = \text{slope}$ $C = \text{intercept}$		
	R^2	q_e ($\frac{\text{mg}}{\text{g}}$)	K_1 ($\frac{1}{\text{min}}$)	R^2	q_e ($\frac{\text{mg}}{\text{g}}$)	K_2 ($\frac{\text{g}}{\text{mg}\cdot\text{min}}$)	R^2	C	K_i ($\frac{\text{mg}}{\text{g}\cdot\text{min}^{0.5}}$)
Pb	0.92	0.016	0.007	1	14.60	7.82	0.93	14.58	0.001
Ni	0.93	0.483	0.028	1	21.74	0.21	0.99	21.28	0.038
Co	0.60	0.260	0.032	1	17.30	0.78	0.75	20.58	0.011
Cd	0.71	0.101	0.014	1	20.75	0.46	0.76	17.23	0.006

3.6. Adsorption Isotherms and Effect of Initial Concentration

Adsorption isotherms describe the interaction between an adsorbing material and an adsorbent. They reveal information related to the adsorption mechanism. Adsorption isotherms indicate the relationships between the equilibrium concentrations of adsorbates in the solid phase (q_e) and in the liquid phase (c_e) at a constant temperature [54,55]. The equilibrium amount of pollutants per unit mass of adsorbent is obtained based on Equation (1).

3.6.1. Langmuir Isotherm

The Langmuir isotherm is a theoretical model assuming that monolayer adsorption occurs at particular homogeneous sites on the surface of an adsorbent and all adsorption sites have equal adsorption energies [56].

The linear forms of the Langmuir equation, which was applied to the experimental data, are expressed by Equation (5) [57]:

$$\frac{c_e}{q_e} = \frac{1}{K_L q_m} + \frac{1}{q_m} c_e \quad (5)$$

where C_0 and C_e (mg/L) are the initial and equilibrium concentrations of heavy metals, q_e (mg/g) denotes the adsorption capacity at the equilibrium, K_L (L/mg) represents the Langmuir isotherm constant and q_m (mg/g) is the maximum adsorption capacity of the adsorbent at equilibrium. K_L and q_m can be obtained from the linear fit of C_e/q_e versus C_e .

3.6.2. Freundlich Isotherm

The Freundlich isotherm model is mostly used to understand the adsorption of metal ions on a heterogeneous surface with multilayer adsorption [58]. It can also define surface heterogeneity and an exponential distribution of active sites and their energy [59]. The linear form of the Freundlich isotherm model is expressed by Equation (6) [60]:

$$\ln q_e = \ln K_F + \left(\frac{1}{n}\right) \ln C_e \quad (6)$$

where q_e (mg/g) is the adsorption capacity at equilibrium, C_e (mg/L) denotes the equilibrium concentration, K_F refers to the Freundlich constant, which is related to the total

adsorption capacity, and n represents the intensity of adsorption. K_F and n are the Freundlich constants and can be obtained from the linear fit of $\ln q_e$ versus $\ln C_e$.

In Equation (10), n is a constant value and controls the deviation from the linear form of adsorption, and it describes the isotherm type in the Freundlich model. If n is between 1 and 10, it indicates the suitability of the adsorption process. The closer this value is to 1, the less important the heterogeneity of the surface is, and the closer it comes to 10, the more important the level of homogenization increases is, and the chemical adsorption overcomes physical adsorption [56].

3.6.3. Dubinin-Radushkevich Isotherm

The Dubinin-Radushkevich (D-R) isotherm model is an empirical model that is usually used to interpret adsorption nature by distributing Gaussian energy on a heterogeneous surface and uses the energy of each adsorbed molecule (E). This model fits the data well for solutes with high and medium concentrations. The linear forms of the D-R adsorption isotherm model can be expressed as Equations (7) and (12), respectively [61]:

$$nq_e = \ln q_m - \beta \varepsilon^2 \quad (7)$$

where q_m (mg/g) is the D-R monolayer capacity, ε represents the Polanyi adsorption potential related to the equilibrium concentration and correlated as Equation (8) and β (mol²/KJ²) denotes a constant related to the adsorption energy, which gives the mean free energy E (kJ/mol) as Equation (9):

$$\varepsilon = RT \ln \left(1 + \frac{1}{C_e} \right) \quad (8)$$

$$E = \frac{1}{\sqrt{2\beta}} \quad (9)$$

Some valuable information about the adsorption process can be obtained from the free energy of the molecule (E). If the value of the adsorption energy is less than 8 kJ, it indicates that the adsorption has occurred physically, and if it is between 8 and 16 KJ/mol, it suggests that the adsorption process has been carried out chemically [62].

In order to interpret the adsorption mechanism, Langmuir, Freundlich and Dubinin-Radushkevich (D-R) adsorption models were tested, and the best isotherm was determined by drawing graphs of the models and comparing their correlation coefficient values. The adsorption isotherm data of the metal ions by *C. zizanioides* root powder are shown in Figure 9. As can be observed in the diagram, the adsorption capacity increases with the increase in the initial metal ion concentrations.

The results for the Langmuir, Freundlich and Dubinin-Radushkevich (D-R) isotherm models are given in Table 4. Based on the correlation coefficient values (R^2), it can certainly be said that the results obtained from the isotherm studies of the biosorption of Pb, Ni, Cd and Co metal ions by *C. zizanioides* root powder are the most compatible with the Freundlich and Dubinin-Radushkevich models. Exceptionally, cadmium followed the Langmuir isotherm model as well. It suggests that cadmium biosorption by *C. zizanioides* root powder is multilayered and more likely to occur physically [63]. The values of n in the Freundlich isotherm model also indicate that the physical adsorption overcomes the chemical adsorption [56]. In addition, considering that the values of E in the D-R model are less than 8 kJ/mol, it can be concluded that the adsorption nature was physical. According to Table 4, the maximum monolayer adsorption capacities obtained from the D-R model were 31.78, 21.52, 26.69 and 27.81 (mg/g) for lead, nickel, cobalt and cadmium, respectively.

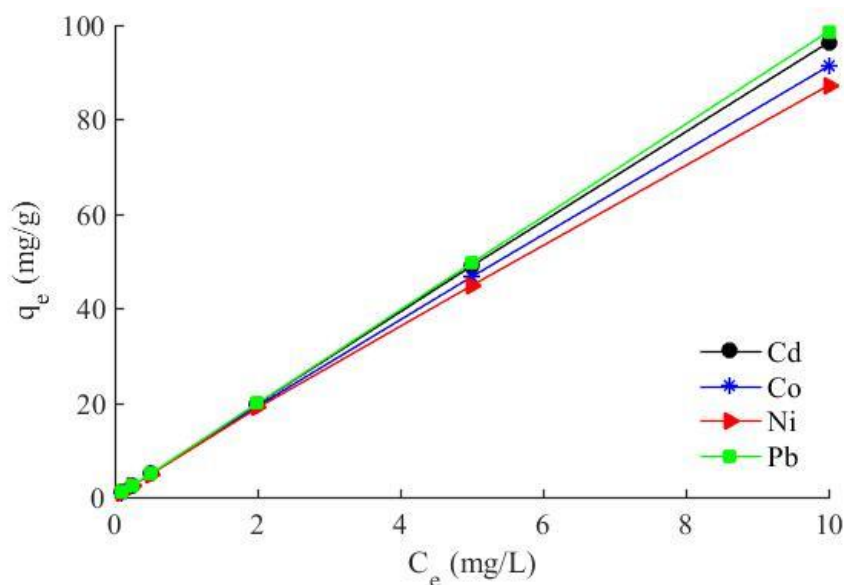


Figure 9. Adsorption isotherms of Pb, Ni, Co and Cd (initial concentrations: 1.46, 2.19, 2.08 and 1.73 mg/L, respectively, adsorbent dosage: 100 mg/L, volume of solution: 100 mL, time: 5 min, T = 298 K, pH = 7.0).

Table 4. Fitting parameters of the isotherm models for the biosorption of lead, nickel, cadmium and cobalt by *C. zizanioides* root powder.

Elements	Langmuir Plot: C_e/q_e vs. C_e $q_m = 1/\text{slope}$ $k_L = \text{slope}/\text{intercept}$			Freundlich Plot: $\ln q_e$ vs. $\ln C_e$ $n = 1/\text{slope}$ $k_F = \exp(\text{intercept})$			Dubinin-Radushkevich Plot: $\ln q_e$ vs. ϵ^2 $q_m = \exp(\text{intercept})$ $E = 1/(2(-\text{slope}))^{0.5}$		
	q_m ($\frac{\text{mg}}{\text{g}}$)	k_L ($\frac{1}{\text{mg}}$)	R^2	n	K_F	R^2	q_m ($\frac{\text{mg}}{\text{g}}$)	E ($\frac{\text{KJ}}{\text{mol}}$)	R^2
Pb	87.33	0.12	0.58	1.04	747.25	0.96	31.78	5	0.98
Ni	91.03	0.24	0.91	1.26	82.70	0.98	21.52	4.1	0.98
Co	78.57	0.25	0.91	1.28	118.96	0.97	26.69	5	0.98
Cd	53.33	0.50	0.97	1.36	256.98	0.97	27.81	5	0.99

3.7. Adsorption Thermodynamics and Effect of Temperature

In a biosorption study, temperature plays an important role in the adsorption process. In adsorption processes, thermodynamic factors such as Gibbs free energy, standard entropy and enthalpy are necessary to be determined in order to describe the feasibility, direction and type of the adsorption process [64].

The Gibbs free energy change (ΔG°) and Van't Hoff equation, which were used to calculate the thermodynamic parameters, can be expressed by Equation (10) and Equation (11), respectively [65]:

$$\Delta G^\circ = -RT \ln K_d \tag{10}$$

$$\ln K_L = \frac{-\Delta H^\circ}{RT} + \frac{\Delta S^\circ}{R} \tag{11}$$

where ΔG° (KJ/mol) is the Gibbs free energy changes, K_L (L/mol) represents the Langmuir constant, T (K) refers to the absolute temperature, R (8.314 J/mol/K) stands for the ideal gas constant, ΔH° (KJ/mol) denotes the enthalpy changes and ΔS° (KJ/K·mol) signifies the entropy changes.

The effect of temperature on the biosorption capacities of the polluting metals by *C. zizanioides* root powder is shown in Figure 10 for two concentrations of each metal ion: the

initial concentrations of the metal ions (a) and 5 (mg/L) (b), respectively. It can clearly be seen that an increase in the temperature reduces the adsorption capacity of the polluting metals, which is more noticeable for nickel.

The results related to the thermodynamics of metal ion biosorption with a *C. zizanioides* root powder biosorbent are presented in Table 5. The negativity of ΔH^0 confirms the exothermicity of the adsorption reaction of the metals by *C. zizanioides* root powder biosorbent, and the negativity of ΔG^0 indicates the possibility and spontaneity of the adsorption reaction [66].

The values of ΔG^0 decreased with increasing temperature from 298 K to 323 K, which shows that the adsorption of the four metals by the *C. zizanioides* root powder biosorbent is more favorable at room temperature than at higher temperatures. Moreover, it shows economic applicability for wastewater treatment.

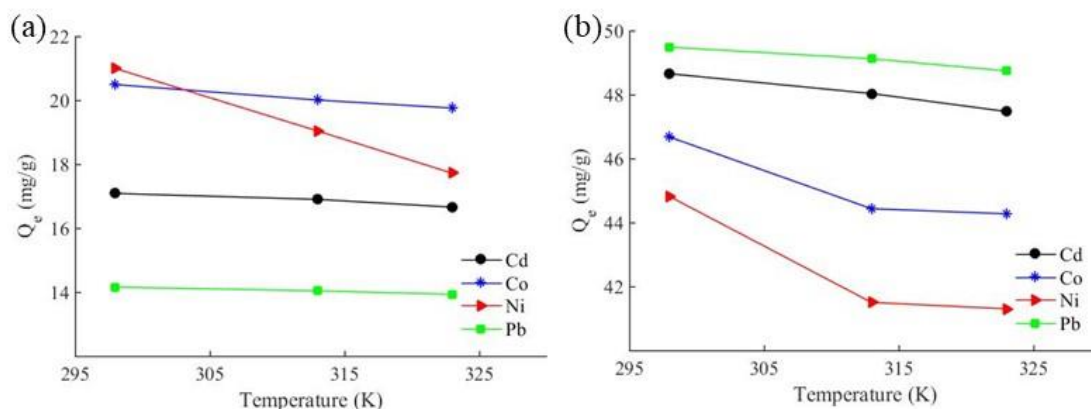


Figure 10. Effect of temperature on the biosorption of Pb, Ni, Co and Cd; (a) initial concentrations of each metal ion: 1.46, 2.19, 2.08 and 1.73 mg/L, respectively, (b) 5 mg/L, adsorbent dosage: 100 mg/L, volume of solution: 100 mL, time: 120 min, T: 298–313–323 K).

In addition, ΔG^0 values greater than -20 kJ/mol suggest the physical adsorption mechanism for the adsorption of the metals on the *C. zizanioides* root powder [67]. The low amount of negative ΔS^0 also indicates a decrease in the degree of freedom of the metal ion adsorption on the *C. zizanioides* root powder [68].

Table 5. The parameters of adsorption thermodynamics.

Adsorbents	C_0 (ppm)	ΔG^0 ($\frac{KJ}{mol}$)			ΔS^0 ($\frac{KJ}{K \cdot mol}$)	ΔH^0 ($\frac{KJ}{mol}$)
		298 K	313 K	323 K		
Pb	1.46	-11.58	-11.53	-11.49	-0.004	-12.723
	5	-16.63	-16.05	-15.67	-0.038	-28.070
Ni	2.19	-13.11	-11.03	-9.64	-0.139	-54.499
	5	-10.68	-10.23	-9.92	-0.030	-19.698
Co	2.08	-15.28	-14.18	-13.46	-0.072	-36.647
	5	-11.86	-11.47	-11.21	-0.026	-19.592
Cd	1.73	-15.79	-15.01	-14.5	-0.051	-31.141
	5	-14.26	-13.96	-13.75	-0.020	-26.358

3.8. Desorption Studies

The desorption studies were performed to investigate the reusability of the biosorbent by conducting several successive adsorption–desorption cycles of metal ions on the biosorbent in order to account for the adsorption economics. One of the valuable features of the adsorbent is its ability to be utilized in several consecutive cycles while maintaining its high adsorption capacity.

C. zizanioides root powder was rinsed with 0.15 M HNO₃ after each adsorption step and was prepared for the next cycle. As shown in Figure 11a, the biosorption rate almost decreased after each cycle. As can be seen, cadmium, Lead and Nickel were well adsorbed on the surface of the biosorbent in the first two cycles, and after that, their adsorption rate decreased. Cobalt was well adsorbed on the biosorbent surface in the first three cycles, and after that, its adsorption rate was lower. All of the metals were adsorbed on the surface of the biosorbent in all four cycles properly. The amount of metal desorption from the biosorbent is also shown in Figure 11b, which demonstrates that the desorption rates of cadmium, cobalt, nickel and lead from the biosorbent increased after each cycle. This suggests that *C. zizanioides* root powder can be utilized for four consecutive cycles and still achieve a high adsorption efficiency.

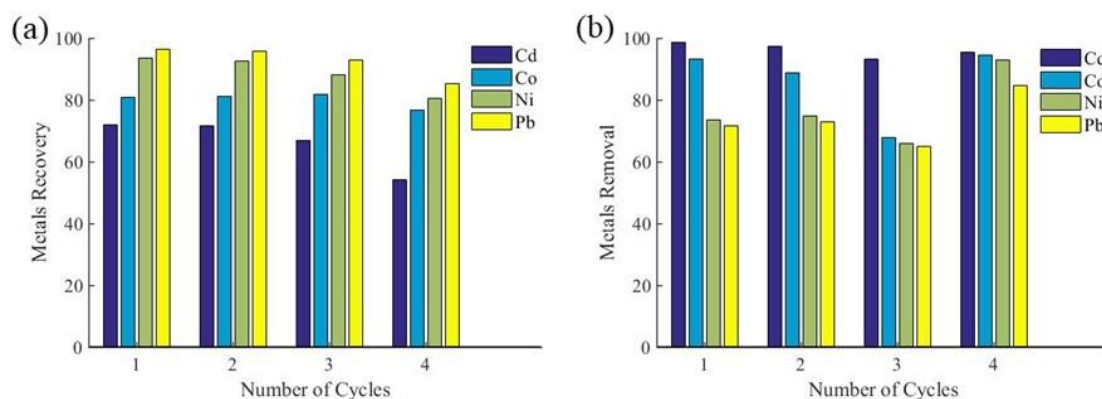


Figure 11. (a) The reusability of *C. zizanioides* root powder in four cycles, (b) metals desorption from *C. zizanioides* root powder in four cycles.

4. Conclusions

In the current study, *C. zizanioides* root powder was used as a biosorbent for testing its ability to remove lead, nickel, cobalt and cadmium from an aqueous solution. *C. zizanioides* root powder was characterized by several analyses and was determined to have a specific surface area of 8.21 m²/g, which is a suitable amount in comparison with other plant biosorbents. Furthermore, it was measured to have an average pore diameter of 7.36 nm.

The present study illustrated that the adsorption isotherms best followed the Freundlich and Dubinin-Radushkevich (D-R) models, which predicted the physical type for the adsorption reactions. Moreover, the kinetic results well fitted the pseudo-second-order kinetic model. The kinetic results also showed that the adsorption process occurred quickly, especially at the beginning of the biosorption process. In addition, according to thermodynamic experiments, the biosorption was an exothermic and spontaneous process.

It was further found that *C. zizanioides* root powder has the ability to separate more than 95 percent of metal ions from an aqueous solution within 5 min, and the maximum adsorption capacities of lead, nickel, cobalt and cadmium were obtained as 31.78, 21.52, 26.69 and 27.81 mg/g, respectively. Desorption studies also showed that the *C. zizanioides* root powder can simply remove the desired metals to a very high amount from the wastewater after four successive cycles.

In conclusion, the current biosorbent (*C. zizanioides* root powder) appears to be a favorable biosorbent, due to its rapid removal and being efficient, economical and applicable for the removal of polluting metal ions from industrial wastewater.

Author Contributions: Conceptualization, S.M. and F.D.A.; methodology, S.M. and F.D.A.; formal analysis, S.M., Z.B., H.S. and R.T.; investigation, S.M.; writing—review and editing, S.M., F.D.A., H.S., Z.B., R.T. and C.B.; funding acquisition, F.D.A. and C.B. All authors have read and agreed to the published version of the manuscript.

Funding: This research received no external funding.

Data Availability Statement: Not applicable.

Conflicts of Interest: The authors declare that they have no conflict of interest.

References

1. Fu, F.; Dionysiou, D.D.; Liu, H. The Use of Zero-Valent Iron for Groundwater Remediation and Wastewater Treatment: A Review. *J. Hazard. Mater.* **2014**, *267*, 194–205. [[CrossRef](#)] [[PubMed](#)]
2. Molinos-Senante, M.; Gómez, T.; Garrido-Baserba, M.; Caballero, R.; Sala-Garrido, R. Assessing the Sustainability of Small Wastewater Treatment Systems: A Composite Indicator Approach. *Sci. Total Environ.* **2014**, *497–498*, 607–617. [[CrossRef](#)] [[PubMed](#)]
3. Maret, W. The Metals in the Biological Periodic System of the Elements: Concepts and Conjectures. *Int. J. Mol. Sci.* **2016**, *17*, 66. [[CrossRef](#)] [[PubMed](#)]
4. JAIN, J.; GAUBA, P. Heavy Metal Toxicity-Implications on Metabolism and Health. *Int. J. Pharma Bio Sci.* **2017**, *8*, 452–460. [[CrossRef](#)]
5. Silva, A.L.O.D.; Barrocas, P.R.; Jacob, S.D.C.; Moreira, J.C. Dietary and Health Effects of Selected Toxic Elements. *Braz. J. Plant Physiol.* **2005**, *17*, 79–93. [[CrossRef](#)]
6. World Health Organization, and WHO. *Guidelines for Drinking-Water Quality*; World Health Organization: Geneva, Switzerland, 2004; Volume 1.
7. Ekramul Mahmud, H.N.M.; Obidul Huq, A.K.; Yahya, R.B. The Removal of Heavy Metal Ions from Wastewater/Aqueous Solution Using Polypyrrole-Based Adsorbents: A Review. *RSC Adv.* **2016**, *6*, 14778–14791. [[CrossRef](#)]
8. Briffa, J.; Sinagra, E.; Blundell, R. Heavy Metal Pollution in the Environment and Their Toxicological Effects on Humans. *Heliyon* **2020**, *6*, e04691. [[CrossRef](#)]
9. Zhang, Y.; Duan, X. Chemical Precipitation of Heavy Metals from Wastewater by Using the Synthetical Magnesium Hydroxy Carbonate. *Water Sci. Technol.* **2020**, *81*, 1130–1136. [[CrossRef](#)]
10. Pang, F.M.; Teng, S.P.; Teng, T.T.; Omar, A.M. Heavy Metals Removal by Hydroxide Precipitation and Coagulation-Flocculation. *Water Qual. Res. J. Can.* **2009**, *44*, 174–182. [[CrossRef](#)]
11. Lewis, A.E. Review of Metal Sulphide Precipitation. *Hydrometallurgy* **2010**, *104*, 222–234. [[CrossRef](#)]
12. Tran, T.K.; Chiu, K.F.; Lin, C.Y.; Leu, H.J. Electrochemical Treatment of Wastewater: Selectivity of the Heavy Metals Removal Process. *Int. J. Hydrogen Energy* **2017**, *42*, 27741–27748. [[CrossRef](#)]
13. Bashir, A.; Malik, L.A.; Ahad, S.; Manzoor, T.; Bhat, M.A.; Dar, G.N.; Pandith, A.H. Removal of Heavy Metal Ions from Aqueous System by Ion-Exchange and Biosorption Methods. *Environ. Chem. Lett.* **2019**, *17*, 729–754. [[CrossRef](#)]
14. Bakalár, T.; Búgel, M.; Gajdošová, L. Heavy Metal Removal Using Reverse Osmosis. *Acta Montan. Slovaca* **2009**, *14*, 250–253.
15. Rath, B.S.; Kumar, P.S. Application of Adsorption Process for Effective Removal of Emerging Contaminants from Water and Wastewater. *Environ. Pollut.* **2021**, *280*, 116995. [[CrossRef](#)] [[PubMed](#)]
16. Younas, F.; Mustafa, A.; Ur, Z.; Farooqi, R.; Wang, X.; Younas, S.; Mohy-ud-din, W.; Hameed, M.A.; Abrar, M.M.; Maitlo, A.A.; et al. Current and Emerging Adsorbent Technologies for Wastewater Treatment: Trends, Limitations, and Environmental Implications. *Water* **2021**, *13*, 215. [[CrossRef](#)]
17. Olya, M.E.; Pirkarami, A.; Mirzaie, M. Adsorption of an Azo Dye in an Aqueous Solution Using Hydroxyl-Terminated Polybutadiene (HTPB). *Chemosphere* **2013**, *91*, 935–940. [[CrossRef](#)]
18. Karnib, M.; Kabbani, A.; Holail, H.; Olama, Z. Heavy Metals Removal Using Activated Carbon, Silica and Silica Activated Carbon Composite. *Energy Procedia* **2014**, *50*, 113–120. [[CrossRef](#)]
19. Pires, C.; Marques, A.P.G.C.; Guerreiro, A.; Magan, N.; Castro, P.M.L. Removal of Heavy Metals Using Different Polymer Matrixes as Support for Bacterial Immobilisation. *J. Hazard. Mater.* **2011**, *191*, 277–286. [[CrossRef](#)]
20. Wang, P.; Du, M.; Zhu, H.; Bao, S.; Yang, T.; Zou, M. Structure Regulation of Silica Nanotubes and Their Adsorption Behaviors for Heavy Metal Ions: PH Effect, Kinetics, Isotherms and Mechanism. *J. Hazard. Mater.* **2015**, *286*, 533–544. [[CrossRef](#)]
21. Ali, R.M.; Hamad, H.A.; Hussein, M.M.; Malash, G.F. Potential of Using Green Adsorbent of Heavy Metal Removal from Aqueous Solutions: Adsorption Kinetics, Isotherm, Thermodynamic, Mechanism and Economic Analysis. *Ecol. Eng.* **2016**, *91*, 317–332. [[CrossRef](#)]
22. Siti Nur, A.A.; Mohd Halim, S.I.; Md Lias Kamal, S.I. Adsorption Prices of Heavy Metals by Low-Cost Adsorbent: A Review. *World Appl. Sci. J.* **2013**, *28*, 1518–1530.
23. Davarnejad, R.; Shoaie, A.; Karimi Dastnayi, Z.; Chehreh, M. Investigation of Affecting Parameters on the Adsorption of Lead (II) from Aqueous Solutions on Henna Powdered Leaves. *Iran. J. Chem. Chem. Eng.* **2020**, *39.2*, 181–189.
24. Tukaram Bai, M.; Venkateswarlu, P. Fixed Bed and Batch Studies on Biosorption of Lead Using Sargassum Tenerrimum Powder: Characterization, Kinetics and Thermodynamics. *Mater. Today Proc.* **2018**, *5*, 18024–18037. [[CrossRef](#)]
25. Zamani Beidokhti, M.; (Omid) Naeeni, S.T.; AbdiGhahroudi, M.S. Biosorption of Nickel (II) from Aqueous Solutions onto Pistachio Hull Waste as a Low-Cost Biosorbent. *Civ. Eng. J.* **2019**, *5*, 447. [[CrossRef](#)]
26. Çelebi, H.; Gök, G.; Gök, O. Adsorption Capability of Brewed Tea Waste in Waters Containing Toxic Lead(II), Cadmium (II), Nickel (II), and Zinc(II) Heavy Metal Ions. *Sci. Rep.* **2020**, *10*, 17570. [[CrossRef](#)]
27. Sayadi, M.H.; Rashki, O.; Shahri, E. Application of Modified Spirulina Platensis and Chlorella Vulgaris Powder on the Adsorption of Heavy Metals from Aqueous Solutions. *J. Environ. Chem. Eng.* **2019**, *7*, 103169. [[CrossRef](#)]

28. Hymavathi, D.; Prabhakar, G. Studies on the Removal of Cobalt(II) from Aqueous Solutions by Adsorption with Ficus Benghalensis Leaf Powder through Response Surface Methodology. *Chem. Eng. Commun.* **2017**, *204*, 1401–1411. [[CrossRef](#)]
29. Zaidi, N.A.H.M.; Lim, B.; Usman, A.; Kooh, M.R.R. Efficient Adsorption of Malachite Green Dye using Artocarpus Odoratissimus Leaves with Artificial Neural Network Modelling. *Desalin. Water Treat.* **2018**, *101*, 313–324. [[CrossRef](#)]
30. Masinire, F.; Adenuga, D.O.; Tichapondwa, S.M.; Chirwa, E.M.N. Phytoremediation of Cr(VI) in wastewater using the vetiver grass (*Chrysopogon zizanioides*). *Miner. Eng.* **2021**, *172*, 107141. [[CrossRef](#)]
31. Kooh, M.R.R.; Thotagamuge, R.; Chau, Y.F.C.; Mahadi, A.H.; Lim, C.M. Machine Learning Approaches to Predict Adsorption Capacity of Azolla Pinnata in the Removal of Methylene Blue. *J. Taiwan Inst. Chem. Eng.* **2022**, *132*, 104134. [[CrossRef](#)]
32. Weshahy, A.R.; Sakr, A.K.; Gouda, A.A.; Atia, B.M.; Somaily, H.H.; Hanfi, M.Y.; Sayyed, M.I.; El Sheikh, R.; El-Sheikh, E.M.; Radwan, H.A.; et al. Selective Recovery of Cadmium, Cobalt, and Nickel from Spent Ni–Cd Batteries using Adogen® 464 and Mesoporous Silica Derivatives. *Int. J. Mol. Sci.* **2022**, *23*, 8677. [[CrossRef](#)] [[PubMed](#)]
33. Lu, H.; Xia, C.; Chinnathambi, A.; Nasif, O.; Narayanan, M.; Shanmugam, S.; Chi, N.T.L.; Pugazhendhi, A.; On-Uma, R.; Jutamas, K.; et al. Optimistic Influence of Multi-metal Tolerant Bacillus Species on Phytoremediation Potential of Chrysopogon Zizanioides on Metal Contaminated Soil. *Chemosphere* **2023**, *311*, 136889. [[CrossRef](#)]
34. Danh, L.T.; Truong, P.; Mammucari, R.; Tran, T.; Foster, N. Vetiver Grass, Vetiveria Zizanioides: A Choice Plant for Phytoremediation of Heavy Metals and Organic Wastes. *Int. J. Phytoremediat.* **2009**, *11*, 664–691. [[CrossRef](#)] [[PubMed](#)]
35. Danh, L.T. Vetiver System Technology for Prevention and Treatment of Polluted Water and Contaminated Land. Vetiver System: A Green Investment For Sustainable Development. In Proceedings of the 6th International Conference on Vetiver, Danang City, Vietnam, 8 May 2015; Volume 6.
36. Truong, P.; Van, T.T.; Pinner, E. *Vetiver System Applications Technical Reference Manual*; The Vetiver Network International: San Antonio, TX, USA, 2008.
37. Truong, P. *Vetiver Grass Technology For Mine Rehabilitation*; Office of the Royal Development Projects Board: Bangkok, Thailand, 1999; Volume 19.
38. Chakravarty, P.; Sarma, N.S.; Sarma, H.P. Biosorption of Cadmium(II) from Aqueous Solution Using Heartwood Powder of Areca Catechu. *Chem. Eng. J.* **2010**, *162*, 949–955. [[CrossRef](#)]
39. Tang, Y.; Chen, L.; Wei, X.; Yao, Q.; Li, T. Removal of Lead Ions from Aqueous Solution by the Dried Aquatic Plant, Lemna Perpusilla Torr. *J. Hazard. Mater.* **2013**, *244–245*, 603–612. [[CrossRef](#)]
40. Farhan, A.M.; Al-Dujaili, A.H.; Awwad, A.M. Equilibrium and Kinetic Studies of Cadmium(II) and Lead(II) Ions Biosorption onto Ficus Carcia Leaves. *Int. J. Ind. Chem.* **2013**, *4*, 24. [[CrossRef](#)]
41. Chakravarty, S.; Mohanty, A.; Sudha, T.N.; Upadhyay, A.K.; Konar, J.; Sircar, J.K.; Madhukar, A.; Gupta, K.K. Removal of Pb(II) Ions from Aqueous Solution by Adsorption Using Bael Leaves (*Aegle marmelos*). *J. Hazard. Mater.* **2010**, *173*, 502–509. [[CrossRef](#)]
42. Villena, J.F.; Domínguez, E.; Heredia, A. Monitoring Biopolymers Present in Plant Cuticles by FTIR Spectroscopy. *J. Plant Physiol.* **2000**, *156*, 419–422. [[CrossRef](#)]
43. Joga Rao, H.; King, P.; Prasanna Kumar, Y. Equilibrium Isotherm, Kinetic Modeling, and Characterization Studies of Cadmium Adsorption in an Aqueous Solution by Activated Carbon Prepared from Bauhinia Purpurea Leaves. *Rasayan J. Chem.* **2018**, *11*, 1376–1392. [[CrossRef](#)]
44. Vilvanathan, S.; Shanthakumar, S. Biosorption of Co(II) Ions from Aqueous Solution Using Chrysanthemum Indicum: Kinetics, Equilibrium and Thermodynamics. *Process Saf. Environ. Prot.* **2015**, *96*, 98–110. [[CrossRef](#)]
45. Li, Q.; Chen, B.; Lin, P.; Zhou, J.; Zhan, J.; Shen, Q.; Pan, X. Adsorption of Heavy Metal from Aqueous Solution by Dehydrated Root Powder of Long-Root Eichhornia Crassipes. *Int. J. Phytoremediation* **2016**, *18*, 103–109. [[CrossRef](#)] [[PubMed](#)]
46. Jain, M.; Garg, V.K.; Kadirvelu, K.; Sillanpää, M. Adsorption of Heavy Metals from Multi-Metal Aqueous Solution by Sunflower Plant Biomass-Based Carbons. *Int. J. Environ. Sci. Technol.* **2016**, *13*, 493–500. [[CrossRef](#)]
47. Süleyman İnan, B.Ö. Sorption of Cobalt and Nickel on Narcissus Tazetta L. Leaf Powder. *J. Turk. Chem. Soc.* **2021**, *8*, 705–714.
48. Abdel-Wahed, M.S.; El-Kalliny, A.S.; Badawy, M.I.; Attia, M.S.; Gad-Allah, T.A. Core Double-Shell MnFe₂O₄@rGO@TiO₂ Superparamagnetic Photocatalyst for Wastewater Treatment under Solar Light. *Chem. Eng. J.* **2020**, *382*, 122936. [[CrossRef](#)]
49. Takeno, N. *Atlas of Eh-PH Diagrams Intercomparison of Thermodynamic Databases*; National Institute of Advanced Industrial Science and Technology: Tokyo, Japan, 2005; Volume 285.
50. Gupta, H.; Gogate, P.R. Intensified Removal of Copper from Waste Water Using Activated Watermelon Based Biosorbent in the Presence of Ultrasound. *Ultrason. Sonochem.* **2016**, *30*, 113–122. [[CrossRef](#)]
51. Bakhtiari, N.; Azizian, S. Adsorption of Copper Ion from Aqueous Solution by Nanoporous MOF-5: A Kinetic and Equilibrium Study. *J. Mol. Liq.* **2015**, *206*, 114–118. [[CrossRef](#)]
52. Thue, P.S.; Sophia, A.C.; Lima, E.C.; Wamba, A.G.N.; de Alencar, W.S.; dos Reis, G.S.; Rodembusch, F.S.; Dias, S.L.P. Synthesis and Characterization of a Novel Organic-Inorganic Hybrid Clay Adsorbent for the Removal of Acid Red 1 and Acid Green 25 from Aqueous Solutions. *J. Clean. Prod.* **2018**, *171*, 30–44. [[CrossRef](#)]
53. Rida, K.; Bouraoui, S.; Hadnine, S. Adsorption of Methylene Blue from Aqueous Solution by Kaolin and Zeolite. *Appl. Clay Sci.* **2013**, *83–84*, 99–105. [[CrossRef](#)]
54. Netpradit, S.; Thiravetyan, P.; Towprayoon, S. Application of ‘Waste’ Metal Hydroxide Sludge for Adsorption of Azo Reactive Dyes. *Water Res.* **2003**, *37*, 763–772. [[CrossRef](#)]

55. Ardejani, F.D.; Badii, K.; Limaee, N.Y.; Shafaei, S.Z.; Mirhabibi, A.R. Adsorption of Direct Red 80 Dye from Aqueous Solution onto Almond Shells: Effect of PH, Initial Concentration and Shell Type. *J. Hazard. Mater.* **2008**, *151*, 730–737. [[CrossRef](#)]
56. Al-Rashdi, B.; Tizaoui, C.; Hilal, N. Copper Removal from Aqueous Solutions Using Nano-Scale Diboron Trioxide/Titanium Dioxide (B₂O₃/TiO₂) Adsorbent. *Chem. Eng. J.* **2012**, *183*, 294–302. [[CrossRef](#)]
57. Langmuir, I. The Constitution and Fundamental Properties of Solids and Liquids. Part II. Liquids. *J. Frankl. Inst.* **1917**, *184*, 721. [[CrossRef](#)]
58. Ayawei, N.; Angaye, S.S.; Wankasi, D.; Dikio, E.D. Synthesis, Characterization and Application of Mg/Al Layered Double Hydroxide for the Degradation of Congo Red in Aqueous Solution. *Open J. Phys. Chem.* **2015**, *5*, 56–70. [[CrossRef](#)]
59. Ayawei, N.; Ekubo, A.T.; Wankasi, D.; Dikio, E.D. Adsorption of Congo Red by Ni/Al-CO₃: Equilibrium, Thermodynamic and Kinetic Studies. *Orient. J. Chem.* **2015**, *31*, 1307–1318. [[CrossRef](#)]
60. Freundlich, H. Über Die Adsorption in Lösungen. *Z. Phys. Chem.* **1907**, *57U*, 385–470. [[CrossRef](#)]
61. Dubinin, M.M. The Equation of the Characteristic Curve of Activated Charcoal. *Dokl. Akad. Nauk. SSSR* **1947**, *55*, 327–329.
62. Ouma, I.L.A.; Naidoo, E.B.; Ofomaja, A.E. Thermodynamic, Kinetic and Spectroscopic Investigation of Arsenite Adsorption Mechanism on Pine Cone-Magnetite Composite. *J. Environ. Chem. Eng.* **2018**, *6*, 5409–5419. [[CrossRef](#)]
63. Wang, J.; Guo, X. Adsorption Isotherm Models: Classification, Physical Meaning, Application and Solving Method. *Chemosphere* **2020**, *258*, 127279. [[CrossRef](#)]
64. Greluk, M.; Hubicki, Z. Kinetics, Isotherm and Thermodynamic Studies of Reactive Black 5 Removal by Acid Acrylic Resins. *Chem. Eng. J.* **2010**, *162*, 919–926. [[CrossRef](#)]
65. Wang, L. Application of Activated Carbon Derived from ‘Waste’ Bamboo Culms for the Adsorption of Azo Disperse Dye: Kinetic, Equilibrium and Thermodynamic Studies. *J. Environ. Manag.* **2012**, *102*, 79–87. [[CrossRef](#)]
66. Massoudinejad, M.; Ghaderpoori, M.; Shahsavani, A.; Jafari, A.; Kamarehie, B.; Ghaderpoury, A.; Amini, M.M. Ethylenediamine-Functionalized Cubic ZIF-8 for Arsenic Adsorption from Aqueous Solution: Modeling, Isotherms, Kinetics and Thermodynamics. *J. Mol. Liq.* **2018**, *255*, 263–268. [[CrossRef](#)]
67. Rashidi Nodeh, H.; Sereshti, H. Synthesis of Magnetic Graphene Oxide Doped with Strontium Titanium Trioxide Nanoparticles as a Nanocomposite for the Removal of Antibiotics from Aqueous Media. *RSC Adv.* **2016**, *6*, 89953–89965. [[CrossRef](#)]
68. Venkatesha, T.G.; Viswanatha, R.; Arthoba Nayaka, Y.; Chethana, B.K. Kinetics and Thermodynamics of Reactive and Vat Dyes Adsorption on MgO Nanoparticles. *Chem. Eng. J.* **2012**, *198–199*, 1–10. [[CrossRef](#)]

Disclaimer/Publisher’s Note: The statements, opinions and data contained in all publications are solely those of the individual author(s) and contributor(s) and not of MDPI and/or the editor(s). MDPI and/or the editor(s) disclaim responsibility for any injury to people or property resulting from any ideas, methods, instructions or products referred to in the content.